The Solid Solution $TmNi_{1-x-y}In_{1+x}$

Mar'yana Lukachuk[a], Yaroslav M. Kalychak[b], and Rainer Pöttgen[a]

[a] Institut für Anorganische und Analytische Chemie and NRW Graduate School of Chemistry, Westfälische Wilhelms-Universität Münster, Corrensstraße 36, D-48149 Münster, Germany
[b] Inorganic Chemistry Department, Ivan Franko National University of Lviv, Kyryla and Mephodiya Street 6, 79005 Lviv/Ukraine

Reprint requests to R. Pöttgen. E-mail: pottgen@uni-muenster.de

Z. Naturforsch. **59b,** 893 – 897 (2004); received April 25, 2004

The thulium nickel indide TmNiIn forms solid solutions $TmNi_{1-x-y}In_{1+x}$. Several samples have been prepared by arc-melting of the elements under argon. The structure of TmNiIn contains two crystallographically different nickel sites. The Ni1 atoms have a trigonal prismatic coordination by indium, while the Ni2 sites have six thulium neighbors in a trigonal prismatic arrangement. The Ni1 sites show defects in the solid solution, while the Ni2 sites have Ni2/In mixing with a maximal occupancy of 32 at.-% indium. The structures of three single crystals of solid solutions have been refined, leading to the compositions $TmNi_{0.88}In_{1.10}$ ($a = 747.06(7)$, $c = 367.8(1)$ pm, $wR2 = 0.0342$, 323 F^2 values, 16 variables), $TmNi_{0.80}In_{1.16}$ ($a = 752.94(7)$, $c = 366.5(1)$ pm, $wR2 = 0.0475$, 503 F^2 values, 16 variables), and $TmNi_{0.76}In_{1.21}$ ($a = 758.4(1)$, $c = 366.68(7)$ pm, $wR2 = 0.0949$, 226 F^2 values, 16 variables). The crystal chemical peculiarities and the differences in chemical bonding are briefly discussed.

Key words: Solid Solution, Crystal Structure, Solid State Synthesis

Introduction

A large number of intermetallic compounds [1] crystallizes with the well known hexagonal ZrNiAl type structure [2 – 4], a ternary ordered version of the Fe_2P type [5]. As an example we present a projection of the TmNiIn [6] structure onto the *xy* plane in Fig. 1. The structure contains two crystallographically independent nickel sites which both have trigonal prismatic coordination: Ni1 by six indium and Ni2 by six thulium atoms. These prisms are capped on the rectangular faces by three further atoms leading to coordination number (CN) 9 for the nickel atoms.

The ZrNiAl type compounds show some crystal chemical peculiarities. In some cases, the symmetry is lowered due to the formation of superstructures or due to a different coloring of the atoms on the subcell sites. The ordering variants known up today are listed in the TYPIX compilation [7] and in two recent publications [8, 9].

Most of the ZrNiAl type or related intermetallics have been characterized on the basis of X-ray powder data. This is not without severe problems, since some compounds studied by single crystal techniques showed either mixed atomic sites and/or small defects on some positions [9 – 12 and ref. therein]. To give two examples, YbAuIn shows solid solutions up to $YbAu_{1.27}In_{0.73}$ [10], and in $Sc_3Rh_{1.594}In_4$ [9] there are

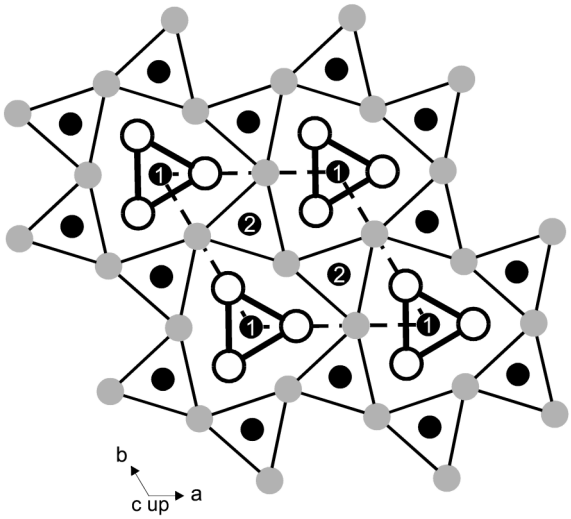

Fig. 1. Projection of the TmNiIn structure onto the *xy* plane. The thulium, nickel, and indium atoms are drawn as large gray, filled, and open circles, respectively. All atoms lie on mirror planes at $z = 0$ (thin lines) and $z = 1/2$ (thick lines). The trigonal prisms around the nickel atoms are emphasized.

Table 1. Lattice parameters of hexagonal $TmNi_{1-x-y}In_{1+x}$ compounds with ZrNiAl type structure.

Compound	a [pm]	c [pm]	c/a	V [nm^3]
TmNiIn [6]	742.6	370.4	0.499	0.1769
TmNiIn [a]	743.2(2)	368.6(1)	0.496	0.1763
$TmNi_{0.88(1)}In_{1.10(1)}$ [b]	747.06(7)	367.8(1)	0.492	0.1778
$TmNi_{0.89}In_{1.11}$ [a]	747.7(2)	367.96(8)	0.492	0.1781
$TmNi_{0.80(1)}In_{1.16(1)}$ [b]	752.94(7)	366.5(1)	0.487	0.1799
$TmNi_{0.74}In_{1.26}$ [a]	753.4(2)	367.33(8)	0.488	0.1806
$TmNi_{0.76(4)}In_{1.21(4)}$ [b]	758.4(1)	366.68(7)	0.483	0.1826
$TmNi_{0.59}In_{1.41}$ [a]	759.3(3)	367.7(1)	0.484	0.1836
$TmNi_{0.35}In_{1.65}$ [a]	766.45(9)	366.96(4)	0.479	0.1867

[a] Lattice parameters from Guinier powder data. The compositions listed here correspond to the starting compositions of the sample preparation; [b] lattice parameters from diffractometer measurements. These compositions have been refined from the single crystal data.

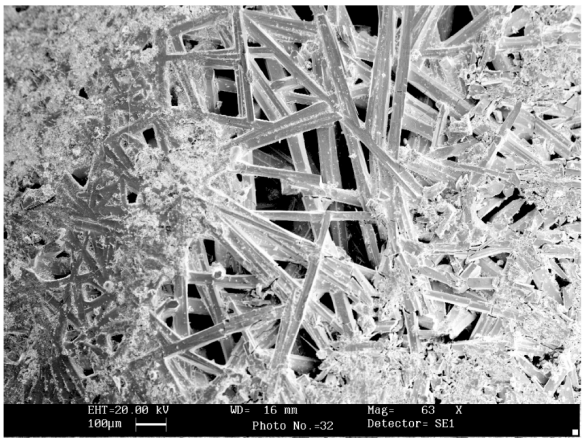

Fig. 2. Scanning electron micrograph of the surface of an arc-melted button of a sample with the starting composition $TmNi_{0.74}In_{1.26}$.

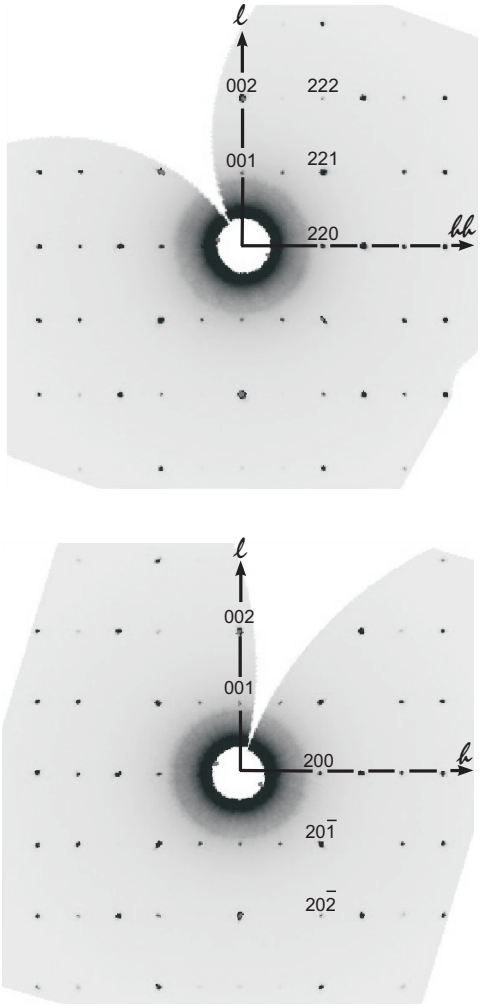

Fig. 3. Reconstructed reciprocal layers *h*0*l* and *hhl* of $TmNi_{0.76}In_{1.21}$.

two rhodium sites with defects, besides the formation of a new superstructure.

Phase analytical investigations in the *RE*–Ni–In systems [13, 14] showed solid solutions $RENi_{1-x}In_{1+x}$ for several rare earth metals. We have studied the thulium based solid solution in more detail by X-ray powder and single crystal data reported herein.

Experimental Section

Synthesis

Starting materials for the preparation of the different $TmNi_{1-x-y}In_{1+x}$ samples were ingots of thulium, nickel wire (⌀ 0.38 mm), and indium tear drops. All elements were supplied by Johnson Matthey with stated purities $> 99.9\%$. The elements were weighed in the atomic ratios listed in Table 1 and arc-melted [15] under an argon pressure of *ca*. 600 mbar. The argon was purified over titanium sponge (900 K), silica gel, and molecular sieves. The product buttons were re-melted three times in order to ensure homogeneity. The total weight losses after the arc-melting procedures were always smaller than 0.5 weight-%. The $TmNi_{1-x-y}In_{1+x}$ samples were all well crystallized. Long needle-shaped single crystals formed on the surface of the arc-melted buttons directly after solidification (Fig. 2). The brittle samples were stable in moist air as compact pieces as well as fine-grained powders. Single crystals exhibited metallic luster.

Scanning electron microscopy

The single crystals investigated on the diffractometers have been analyzed by EDX measurements using a LEICA 420 I scanning electron microscope with TmF_3, Ni, and InAs as standards. No impurity elements were detected. The anal-

Empirical formula	$TmNi_{0.88(1)}In_{1.10(1)}$	$TmNi_{0.80(1)}In_{1.16(1)}$	$TmNi_{0.76(4)}In_{1.21(4)}$
Molar mass	346.32 g/mol	349.28 g/mol	352.29 g/mol
Unit cell dimensions	see Table 1	see Table 1	see Table 1
Calculated density	9.71 g/cm^3	9.67 g/cm^3	9.61 g/cm^3
Crystal size	$10\times20\times40$ μm^3	$40\times50\times60$ μm^3	$20\times40\times60$ μm^3
Detector distance	–	–	60 mm
Exposure time	–	–	14 min
ω Range; increment	–	–	$0-180^\circ$; 1.0°
Integr. param. A, B, EMS	–	–	14.0; 4.0; 0.010
Transm. ratio (max/min)	1.46	1.48	1.96
Absorption coefficient	54.1 mm^{-1}	53.5 mm^{-1}	52.8 mm^{-1}
F(000)	442	445	448
θ Range	3° to 35°	3° to 42°	3° to 30°
Range in *hkl*	±12, ±12, ±5	±14, ±14, ±6	±10, ±10, ±5
Total no. reflections	3096	3162	1895
Independent reflections	323 ($R_{int}=0.0539$)	503 ($R_{int}=0.0460$)	226 ($R_{int}=0.0361$)
Reflections with $I>2\sigma(I)$	316 ($R_{sigma}=0.0234$)	486 ($R_{sigma}=0.0227$)	225 ($R_{sigma}=0.0154$)
Data / parameters	323 / 16	503 / 16	226 / 16
Goodness-of-fit on F^2	1.072	1.081	1.311
Final R indices $[I>2\sigma(I)]$	$R1=0.0174$	$R1=0.0215$	$R1=0.0405$
	$wR2=0.0340$	$wR2=0.0463$	$wR2=0.0949$
R Indices (all data)	$R1=0.0184$	$R1=0.0239$	$R1=0.0405$
	$wR2=0.0342$	$wR2=0.0475$	$wR2=0.0949$
Extinction coefficient	0.0065(6)	0.0136(8)	0.019(3)
Flack parameter	0.03(2)	0.00(2)	0.03(7)
Largest diff. peak and hole	0.94 / −1.44 e/Å^3	1.89 / −2.33 e/Å^3	2.74 / −5.18 e/Å^3

Table 2. Crystal data and structure refinement for $TmNi_{0.88(1)}In_{1.10(1)}$, $TmNi_{0.80(1)}In_{1.16(1)}$, and $TmNi_{0.76(4)}In_{1.21(4)}$ (ZrNiAl type structure, space group $P62m$, $Z=3$).

Atom	Wyckoff position	Occupancy	x	y	z	U_{11}	U_{22}	U_{33}	U_{12}	U_{eq}
$TmNi_{0.88(1)}In_{1.10(1)}$										
Tm	3*f*	100	0.59195(6)	0	0	131(2)	223(2)	97(2)	111(1)	140(1)
Ni1	1*a*	92(1)	0	0	0	89(7)	U_{11}	115(11)	45(4)	98(6)
Ni2/In2	2*d*	86(1)/14(1)	2/3	1/3	1/2	80(5)	U_{11}	150(7)	40(2)	103(4)
In1	3*g*	100	0.25472(8)	0	1/2	87(2)	100(3)	131(3)	50(1)	105(1)
$TmNi_{0.80(1)}In_{1.16(1)}$										
Tm	3*f*	100	0.40725(6)	0	0	174(1)	355(3)	99(1)	178(1)	189(1)
Ni1	1*a*	87(1)	0	0	0	104(6)	U_{11}	121(9)	52(3)	110(5)
Ni2/In2	2*d*	76(1)/24(1)	1/3	2/3	1/2	77(3)	U_{11}	172(5)	39(2)	109(3)
In1	3*g*	100	0.74677(8)	0	1/2	96(1)	105(2)	146(2)	52(1)	115(1)
$TmNi_{0.76(4)}In_{1.21(4)}$										
Tm	3*f*	100	0.4054(3)	0	0	193(7)	548(13)	118(6)	274(7)	247(6)
Ni1	1*a*	90(5)	0	0	0	161(35)	U_{11}	141(46)	80(18)	154(30)
Ni2/In2	2*d*	68(4)/32(4)	1/3	2/3	1/2	77(17)	U_{11}	205(26)	38(8)	119(16)
In1	3*g*	100	0.7478(3)	0	1/2	100(8)	145(11)	164(11)	72(6)	131(6)

Table 3. Atomic coordinates and anisotropic displacement parameters (pm^2) for $TmNi_{0.88(1)}In_{1.10(1)}$, $TmNi_{0.80(1)}In_{1.16(1)}$, and $TmNi_{0.76(4)}In_{1.21(4)}$. U_{eq} is defined as one third of the trace of the orthogonalized U_{ij} tensor. The anisotropic displacement factor exponent takes the form: $-2\pi^2[(ha^*)^2U_{11}+\ldots+2hka^*b^*U_{12}]$. $U_{13}=U_{23}=0$.

yses were in agreement with the compositions refined from the single crystal data (see below).

X-ray film data and structure refinement

All samples were characterized through Guinier powder patterns. The Guinier camera was equipped with an image plate system (Fujifilm–BAS1800) and Cu-K$_{\alpha1}$ radiation. α-Quartz ($a=491.30$, $c=540.46$ pm) was used as an internal standard. The hexagonal lattice parameters (Table 1) were refined by least-squares fits of the Guinier data. The correct indexing was ensured through intensity calculations [16], using the atomic parameters obtained from the structure refinements.

Small irregular or needle-shaped crystals were selected from the different samples and first examined on a Buerger precession camera (equipped with an image plate and white Mo radiation) in order to establish the suitability for intensity data collection. Single crystal intensity data of $TmNi_{0.88}In_{1.10}$ and $TmNi_{0.80}In_{1.16}$ were collected at room temperature by use of a four-circle diffractometer (CAD4) with graphite monochromatized Mo-K$_\alpha$ radiation and a scintillation counter with pulse-height discrimination. The data set of the $TmNi_{0.76}In_{1.21}$ crystal was collected on a STOE IPDS-II diffractometer with monochromated Mo-K$_\alpha$ radiation in oscillation mode. All crystallographic data and details for the data collections are listed in Table 2.

Tm:	4	Ni2/In2	291.6	Ni1:	6	In1	264.6	In1:	2	Ni1	264.6
	1	Ni1	304.8		3	Tm	304.8		2	Ni2/In2	283.0
	2	In1	311.9	Ni2/In2:	3	In1	283.0		2	Tm	311.9
	4	In1	323.9		6	Tm	291.6		4	Tm	324.0
	2	Tm	367.8						2	In1	329.6
	4	Tm	392.0						2	In1	367.8

Table 4. Interatomic distances (pm) in $TmNi_{0.88(1)}In_{1.10(1)}$. Standard deviations are all equal or less than 0.1 pm. All distances within the first coordination spheres are listed.

The isotypism of the three compounds with the ZrNiAl type was already evident from the X-ray powder data. The atomic positions of isotypic YbAuIn [10] were taken as starting values and the structures were refined with anisotropic displacement parameters for all atoms using SHELXL-97 (full-matrix least-squares on F^2) [17]. Refinement of the correct absolute structure was ensured through refinement of the Flack parameter [18, 19]. In order to check for the solid solution, the occupancy parameters of the two nickel sites and the indium site were refined in a separate series of least-square cycles along with the displacement parameters. For each crystal the 3*g* indium site was fully occupied. In contrast, the 1*a* Ni1 site showed smaller occupancy parameters. Since the nickel atoms have the lowest scattering power in these compounds, this can only be rationalized with nickel defects. The 2*d* Ni2 sites showed higher occupancies which can only be explained through Ni/In mixing. Thus, in the final cycles these two positions were refined with free occupancy parameters for Ni1 and Ni/In mixing for the 2*d* sites leading to the compositions listed in Table 2. The structures smoothly converged to the residuals listed in Table 2 and the final difference Fourier synthesis revealed no significant residuals peaks. The atomic parameters and the interatomic distances are listed in Tables 3 and 4. Further details on the structure refinements are available.*

As is evident from the anisotropic displacement parameters, especially for $TmNi_{0.76}In_{1.21}$ (Table 3), the indides show the typical features we observed also for the subcells of HfRhSn [8] or ScPtSn [20]. We have therefore carefully analyzed this crystal on the image plate diffractometer in order to check for diffuse scattering or superstructure reflections. The reciprocal layers *h*0*l* and *hhl* are presented in Fig. 3 as examples. No indications for a cell enlargement have been observed.

Discussion

The thulium nickel indide TmNiIn forms solid solutions $TmNi_{1-x-y}In_{1+x}$. Various samples within this range of composition have been prepared and investigated on the basis of X-ray powder and single crystal data. First we should discuss the course of the lattice parameters. As is evident from Table 1 and Fig. 4, the *a* lattice parameter significantly increases and the *c* lattice parameter slightly decreases if some of the smaller nickel atoms (metallic radius 125 pm) are substituted by indium atoms (163 pm metallic radius [21]). The nickel/indium substitution takes place in the trigonal prisms formed by the large thulium atoms (175 pm metallic radius). The height of these prisms is determined by the size of the thulium atoms, while the width of the prisms depends on the size of the centering atoms. This explains the course of the lattice parameters. Since *a* increases more strongly than *c* decreases, we observe an increase of the cell volume upon nickel/indium substitution at the 2*d* Ni2 position. This behavior is similar to that of the solid solutions $RENi_{1-x}In_{1+x}$ (RE = Gd – Er) [11, 12].

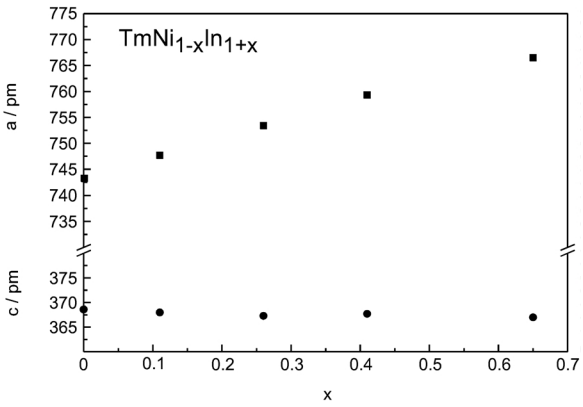

Fig. 4. Course of the unit cell parameters for the solid solutions $TmNi_{1-x}In_{1+x}$ (in this plot we do not account for the small nickel defects on the 1*a* positions, since the bulk samples have been prepared with the *x* values given in the plot.). The size of the symbols corresponds approximately to the standard deviation of the cell parameters.

In contrast to the X-ray powder investigations of [11], our single crystal data revealed interesting additional information. For each crystal the Ni1 position shows small defects. Since the nickel atoms have the smallest scattering power in these compounds, mixing with other atoms can definitively be excluded. Furthermore, the single crystal data show anisotropic displacements for the Ni2/In2 and Tm atoms. While

*Details may be obtained from: Fachinformationszentrum Karlsruhe, D-76344 Eggenstein-Leopoldshafen (Germany), by quoting the Registry No's. CSD–414076 ($TmNi_{0.88}In_{1.10}$), CSD–414075 ($TmNi_{0.80}In_{1.16}$), and CSD–414074 ($TmNi_{0.76}In_{1.21}$).

the Ni2/In2 atoms centering these prisms show alterations along the *c* axis (enhanced U_{33} parameters), the Tm atoms show larger U_{22} parameters. The ratios U_{22}/U_{11} for the Tm and U_{33}/U_{11} for the Ni2/In2 sites continuously increase from the $TmNi_{0.88}In_{1.10}$ to the $TmNi_{0.76}In_{1.21}$ crystal. Similar structural features have been observed for the subcell structures of HfRhSn [8], ZrPtGa [4], and ScPtSn [20]. However, for the crystals of the solid solution $TmNi_{1-x-y}In_{1+x}$, no superstructure reflections have been observed (Fig. 3). Finally it is interesting to compare the solid solutions $TmNi_{1-x-y}In_{1+x}$ and $YbAu_{1+x}In_{1-x}$. For the latter the so far highest *x* value was observed for $YbAu_{1.27}In_{0.73}$ on the basis of a single crystal structure refinement [10]. However, there is a significant difference with respect to the $TmNi_{1-x-y}In_{1+x}$ system reported here. In $YbAu_{1.27}In_{0.73}$ the 3*g* site shows mixed occupancy by 27% Au and 73% In, while it is fully occupied by In atoms in $TmNi_{1-x-y}In_{1+x}$.

Acknowledgments

We thank Dipl.-Ing. U. Ch. Rodewald for the intensity data collections and H.-J. Göcke for the work at the scanning electron microscope. This work was financially supported by the Deutsche Forschungsgemeinschaft. M. L. is indebted to the NRW Graduate School of Chemistry for a PhD stipend.

[1] P. Villars, L. D. Calvert, Pearson's Handbook of Crystallographic Data for Intermetallic Phases, Second Edition, American Society for Metals, Materials Park, OH 44073 (1991), and desk edition (1997).
[2] A. E. Dwight, M. H. Mueller, R. A. Conner (Jr.), J. W. Downey, H. Knott, Trans. Met. Soc. AIME **242**, 2075 (1968).
[3] P. I. Krypyakevich, V. Ya. Markiv, E. V. Melnyk, Dopov. Akad. Nauk. Ukr. RSR, Ser. A 750 (1967).
[4] M. F. Zumdick, R.-D. Hoffmann, R. Pöttgen, Z. Naturforsch. **54b**, 45 (1999).
[5] S. Rundqvist, F. Jellinek, Acta Chem. Scand. **13,** 425 (1959).
[6] R. Ferro, R. Marazza, G. Rambaldi, Z. Metallkd. **65**, 37 (1974).
[7] E. Parthé, L. Gelato, B. Chabot, M. Penzo, K. Cenzual, R. Gladyshevskii, TYPIX – Standardized Data and Crystal Chemical Characterization of Inorganic Structure Types. Gmelin Handbook of Inorganic and Organometallic Chemistry, 8th ed., Springer, Berlin (1993).
[8] M. F. Zumdick, R. Pöttgen, Z. Kristallogr. **214**, 90 (1999).
[9] M. Lukachuk, V. I. Zaremba, R.-D. Hoffmann, R. Pöttgen, Z. Naturforsch. **59b**, 182 (2004).
[10] R. Pöttgen, Y. Grin, Z. Kristallogr. **Suppl. 12**, 136 (1997).
[11] Yu. B. Tyvanchuk, Ya. M. Kalychak, Ł. Gondek, M. Rams, A. Szytuła, Z. Tomkowicz, J. Magn. Magn. Mater. **277**, 368 (2004).
[12] Ł. Gondek, A. Szytuła, S. Baran, M. Rams, J. Hernandez-Velasco, Yu. B. Tyvanchuk, J. Magn. Magn. Mater. **278**, 392 (2004).
[13] Ya. M. Kalychak, V. I. Zaremba, Yu. B. Tyvanchuk, 6th International Conference on the Crystal Chemistry of Intermetallic Compounds, Lviv, Ukraine, 77 (1995).
[14] Ya. M. Kalychak, J. Alloys Compd. **262 – 263**, 341 (1997).
[15] R. Pöttgen, Th. Gulden, A. Simon, GIT-Laborfachzeitschrift **43**, 133 (1999).
[16] K. Yvon, W. Jeitschko, E. Parthé, J. Appl. Crystallogr. **10**, 73 (1977).
[17] G. M. Sheldrick, SHELXL-97, Program for Crystal Structure Refinement, University of Göttingen, Germany (1997).
[18] H. D. Flack, G. Bernadinelli, Acta Crystallogr. **55A**, 908 (1999).
[19] H. D. Flack, G. Bernadinelli, J. Appl. Crystallogr. **33**, 1143 (2000).
[20] R. Mishra, R. Pöttgen, R.-D. Hoffmann, H. Trill, B. D. Mosel, H. Piotrowski, M. F. Zumdick, Z. Naturforsch. **56b**, 589 (2001).
[21] J. Emsley, The Elements, Oxford University Press, Oxford (1999).